Analysis of Side Lobes Cancellation Methods for BOCcos(n,m) Signals

M. Navarro-Gallardo
G. López-Risueño
and M. Crisci
ESA/ESTEC
Noordwijk, The Netherlands

G. Seco-Granados
SPCOMNAV
Universitat Autònoma de Barcelona
Bellaterra (Barcelona), Spain

Abstract—The next generation of Global Navigation Satellite Systems (GNSS) are implementing Binary Offset Carrier (BOC) modulation. These signals were expected to provide not only better precision in the estimation of the signal's delay and phase but also more robustness to multipath effects. The advantage of BOC signals is that the main lobe of the correlation is very narrow although they present side lobes. For high-order signals, the amplitude of the side lobes can be similar to the amplitude of the main one or even exceed it under specific scenarios. One kind of techniques that mitigates the ambiguity problem is called Side Lobes Cancellation (SLC). The idea of these methods is to see the BOC signal as a sum of different sub-signals which are orthogonal in time domain. These techniques compute the cross-correlation function between the incoming BOC signal and the sub-signals obtaining sub-correlations functions and then they combine them in order to achieve an unambiguous correlation. Although, this kind of techniques are able to work with any kind of BOC signals, there are very few papers that deal with high-order BOC signals or even with BOCcos signals. This paper presents a thorough study about Side Lobes Cancellation methods (SLC), with special emphasis on high-order BOC signals. The main purpose of this paper is to demonstrate the behaviour on Side lobe Cancellation methods (SLC) for high-order BOCcos signals.

Index Terms—Ambiguity, BOC, BOCcos, detection probability, false detection probability, side lobes,

I. INTRODUCTION

Currently, Europe is developing a new GNSS (Global Navigation Satellite System) named GALILEO. This system uses BOC (Binary Offset Carrier) signals, which rely on the use of a subcarrier with a higher frequency than the chip rate. These signals were expected to provide not only better precision in the estimation of the signals delay and phase but also more robustness to multipath effects (i.e. the effect whereby the transmitted signal reaches the receiver through different paths which experience different delays and attenuations). These contributions are combined in reception with the direct signal causing an error in the estimation of the position. BOC signals will also be used in the upgrade of the GPS system and in the future Chinese (COMPASS/BEIDOU) and Indian (GAGAN) systems. The advantage of BOC signals is that the main lobe of the correlation is very narrow although it presents some side lobes. For signals of high order, the amplitude of the side lobes can be similar to the amplitude of the main lobe or even exceed it. This effect is produced in environments with strong multipath effects, high thermal noise and/or high interference. The fact that the side lobes have similar values to the main one can produce a synchronization error, where a side lobe is taken as the main lobe, and thus producing an error in the computation of the position. The error can be on the order of tens of meters, what is unacceptable for the user.

Several methods have been proposed in order to mitigate the ambiguity: the bump-jump (BJ) method [1] which provides the classical Early-Late gate with two additional gates, Very Early (VE) and Very Late (VL), intended to check the amplitude of adjacent peaks with respect to the Prompt (P) gate. Another method is the BPSK-like [2] which changes the shape of the BOC correlation into BPSK correlation. It achieves a unambiguous correlation but it loses the properties of the BOC signals. In [3] a novel method is proposed. Its main idea is to eliminate the side lobes in the correlation. The handicap of this method is that it only works with BOCsin(n,n) signals. In the same way, in [4] the authors present a unambiguous technique which is named as General Removing Ambiguity via Side lobe Suppression (GRASS) for BOCsin(n,m) signals.

There is another kind of unambiguous methods based on three loops as the Dual Estimate Tracking (DET) [5]: PLL for the phase delay, DLL for the code delay and the new one for the subcarrier delay. It means that, the code and subcarrier delays could be different. In [6] a study shows the behaviour of these method in a high-order BOC signal, specifically for a BOCcos(15,2.5). The results are quite interesting. They demonstrate that, these methods have a good behaviour even in a urban scenario.

Recently, another kind of techniques, called Side Lobe Cancellation (SLC), that are also able to achieve a unambiguous correlation with BOCcos(n,m) signals [7] [8] have appeared. The idea of these methods is to see the correlation function of the BOC signal as sub-correlations functions and then, make a recombination of them in a determined way in order to achieve a unambiguous correlation. This recombination is done using non linear operations. Therefore, the noise power grows. There are almost no studies on the filtered effect and even the impact of the noise in terms of C/No. In addition, the few studies that can be found, only deal with the BOCcos(1,1) signal and BOCcos(2,1). In this paper a complete analysis of these techniques using a higher-order BOCcos signal is presented.

The study is focused on BOCcos(15,2.5) signal.

The remainder of this paper is organized as follows. In Section II, the signal model used with the SLC methods and the BOCcos(15,2.5) are presented. Section III shows the correlation of the new methods, it means the methods themselves. The results of the filtered effect and impact of the noise are shown in Section IV, as well as, the probabilities of detection and false alarm. Finally Section V denotes the conclusions.

II. BOC SIGNAL

The Binary Offset Carrier (BOC) signals have been chosen by the Galileo system, the upgrade of the GPS system, in the future Chinese (COMPASS/BEIDOU) and Indian (GAGAN) systems. Usually, the BOC signals are denoted as BOC(f_s, f_c), where f_s refers to the subcarrier frequency, and f_c is the chip rate. Chip is called to the different values of the pseudo code. In GNSS another nomenclature is used: BOC(n,m), which is interpreted as $n = f_s/f_{RF}$ and $m = f_c/f_{RF}$, where f_{RF} is fundamental frequency, i.e. $f_{RF} = 1.023MHz$.

There are two types of BOC signals: BOCsin(n,m) and BOCcos(n,m), the difference between them is the phase in the subcarrier, which can be expressed as

$$BOC\sin\ Subcarrier = \text{sgn}[\sin(\tfrac{2\pi kt}{T_c})] \\ BOC\cos\ Subcarrier = \text{sgn}[\cos(\tfrac{2\pi kt}{T_c})] \tag{1}$$

for BOCsin and BOCcos. Where sgn is the sign operator and T_c is the chip time. Both types of signals are characterized by the ratio between the carrier and subcarrier, (i.e. the ratio between n and m), which is defined as

$$k = n/m \tag{2}$$

Due to the shape of the BOC chips, the spectrum shape changes with respect to the BPSK modulation used in GPS. The spectrum of a BOC signal is characterized by two main lobes separated a certain distance from the center frequency [9]. Furthermore, the autocorrelation also changes: side lobes appear. In Fig.1 the spectrum and the correlation of the BOCcos(15,2.5) signal can be seen. It is noteworthy the number of side lobes in the correlation as well as the high value of the closest to the principal.

A. Signal model

A BOC(n,m) signal can be expressed as a combination of basic signals as

$$S_{\sin}(t) = \sum_{m=0}^{2k-1} s_{\sin}^m(t) \\ S_{\cos}(t) = \sum_{m=0}^{4k-1} s_{\cos}^m(t) \tag{3}$$
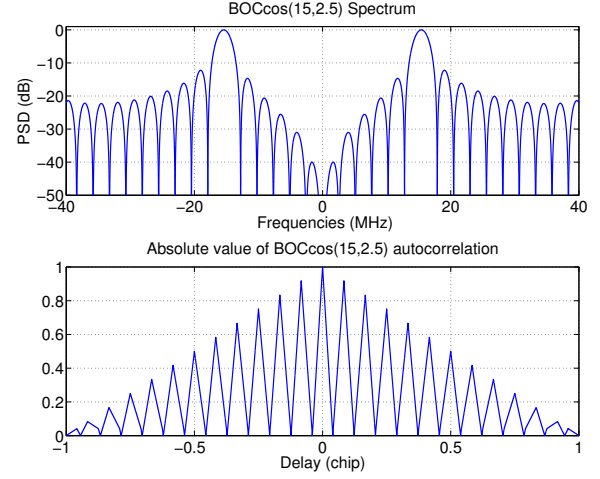
Fig. 1. Spectrum and autocorrelation of BOCcos(15,2.5) signal

for BOCsin and BOCcos. These basic signals can be expressed as the sum of basic orthogonal pulses as

$$s_{\sin}^m(t) = \sum_{i=-\infty}^{\infty} c_i(-1)^m p_{Tsc_{sin}}(t - iT_c - mT_{sc}) \\ for \quad m = 0, 1, ..., 2k - 1 \\ s_{\cos}^m(t) = \sum_{i=-\infty}^{\infty} c_i(-1)^{\lceil \frac{m}{2} \rceil} p_{Tsc_{cos}}(t - iT_c - m\tfrac{T_{sc}}{2}) \\ for \quad m = 0, 1, ...4k - 1 \tag{4}$$

for BOCsin and BOCcos. Where c_i is the i-th chip, T_c is the chip time, T_{sc} is defined by $T_{sc} = \frac{T_c}{2k}$, $p_{Tsc_{sin}}$ and $p_{Tsc_{cos}}$ are defined as

$$p_{Tsc_{\sin}}(t) = \begin{cases} 1 & 0 \le t \le T_{sc} \\ 0 & otherwise \end{cases} \\ p_{Tsc_{\cos}}(t) = \begin{cases} 1 & 0 \le t \le \frac{T_{sc}}{2} \\ 0 & otherwise \end{cases} \tag{5}$$

The steps in order to get these basic signals and pulses can be seen in Fig.2 for a BOCsin(2,1) and in Fig.3 for BOCcos(2.1). It should be noted that, for BOCcos signals $4k$ of basic signals are needed and for BOCsin signals only $2k$ of basic signals are needed. In both cases the basic pulses are orthogonal to each other.

III. CORRELATIONS

This section introduces the BOC signal correlation through basic correlations or sub-correlations formed by the basic signals presented in the previous section.

A. SLC methods

The autocorrelation function for BOCcos signal can be expressed as

$$R_{\cos}(\tau) = \int_0^T S_{cos}(t) S_{cos}(t - \tau) \tag{6}$$
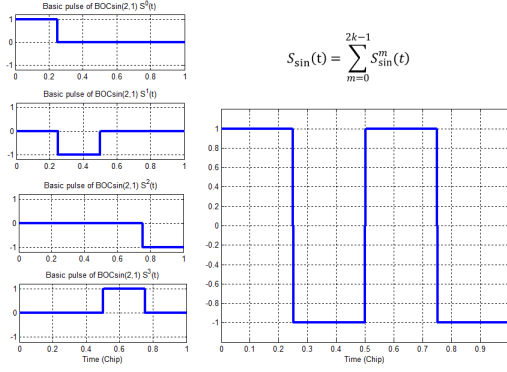
Fig. 2. Generation of BOCsin(2,1) from the basic pulses
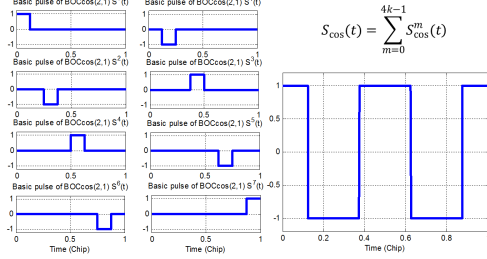
Fig. 3. Generation of BOCcos(2,1) from the basic pulses

Using the form of basic-correlations achieved in Eq(3) for BOCcos signals, the Eq(6) can be expressed as

$$
\begin{aligned}
R_{\cos}(\tau) = & \\
\int_0^T & \left(\sum_{i=-\infty}^{\infty} \sum_{l=0}^{4k-1} (-1)^{\lceil \frac{l}{2} \rceil} c_i p_{Tsc_{cos}}(t - iT_c - l\tfrac{T_{sc}}{2}) \right) \\
& \left(\sum_{j=-\infty}^{\infty} \sum_{m=0}^{4k-1} (-1)^{\lceil \frac{m}{2} \rceil} c_j p_{Tsc_{cos}}(t - \tau - jT_c - m\tfrac{T_{sc}}{2}) \right) dt = \\
\sum_{m=0}^{4k-1} & \sum_{l=0}^{4k-1} (-1)^{\lceil \frac{l}{2} \rceil + \lceil \frac{m}{2} \rceil} \int_0^T \left(\sum_{i=-\infty}^{\infty} c_i p_{Tsc_{cos}}(t - iT_c - l\tfrac{T_{sc}}{2}) \right) \\
& \left(\sum_{j=-\infty}^{\infty} c_j p_{Tsc_{cos}}(t - \tau - jT_c - m\tfrac{T_{sc}}{2}) \right) dt \\
R_{\cos}(\tau) = & \sum_{m=0}^{4k-1} \sum_{l=0}^{4k-1} (-1)^{\lceil \frac{l}{2} \rceil + \lceil \frac{m}{2} \rceil} \Lambda_{cos}(\tau - (l-m)\tfrac{T_{sc}}{2}) \\
R_{\cos}(\tau) = & \sum_{m=0}^{4k-1} R_{\cos}^m(\tau)
\end{aligned}
$$

$$(7)$$

where

$$
R_{\cos}^m(\tau) = \sum_{l=0}^{4k-1} (-1)^{\lceil \frac{l}{2} \rceil + \lceil \frac{m}{2} \rceil} \Lambda_{cos}(\tau - (l-m)\frac{T_{sc}}{2}) \quad (8)
$$

is the correlation function between the m-th sub-carrier pulse and the BOC signal and $\Lambda_{cos}(\tau)$ is defined as

$$
\Lambda_{cos}F = \begin{cases} \frac{T_{sc}}{2} - |\tau|, & |\tau| \leq \frac{T_{sc}}{2} \\ 0, & otherwise \end{cases} \quad (9)
$$

Applying the same process for a BOCsin signal, results

$$
R_{\sin}^m(\tau) = \sum_{l=0}^{2k-1} (-1)^{l+m} \Lambda_{sin}(\tau - (l-m)T_{sc}) \quad (10)
$$

where Λ_{sin} is defined as

$$
\Lambda_{sin} = \begin{cases} T_{sc} - |\tau|, & |\tau| \leq T_{sc} \\ 0, & otherwise \end{cases} \quad (11)
$$

Up to now, the capability of express the BOC signals and, the most important, the BOC correlation functions as the sum of basic signals and and basic correlations has been shown.

B. SLC correlation

The SLC methods are based on the same basic combination in order to achieve a unambiguous correlation [7]. The goal is that, an unambiguous correlation can be achieved using a special combination of the partials correlations. Looking at the partial correlations separately, it can be seen that R_{sin}^0 and R_{sin}^{2k-1} are symmetric to each other other around $\tau = 0$ for BOCsin signals. The same applies for BOCcos using the partials correlations R_{cos}^0 and R_{cos}^{4k-1}. Fig.4 shows these basic correlations of BOCcos(15,2.5) signal. The SLC methods use the following basic combination

$$
\begin{aligned}
R_{\cos}^{Basic}(\tau) = & \\
& \left(|R_{\cos}^0(\tau)| + |R_{\cos}^{4k-1}(\tau)| - |R_{\cos}^0(\tau) - R_{\cos}^{4k-1}(\tau)| \right)
\end{aligned} \quad (12)
$$

for BOCcos signals and

$$
\begin{aligned}
R_{\sin}^{Basic}(\tau) = & \\
& \left(|R_{\sin}^0(\tau)| + |R_{\sin}^{2k-1}(\tau)| - |R_{\sin}^0(\tau) - R_{\sin}^{2k-1}(\tau)| \right)
\end{aligned} \quad (13)
$$

for BOCsin signals in order to achieve a unambiguous correlation. An example of this basic combination of BOC-cos(15,2.5) is shown in Fig.5. It should be noted that this basic combination only uses two partial correlations. Therefore, as the order of the BOC signal increase the input-used power decrease. For instance, when a BOCcos(15,2.5), i.e. 24 sub-correlations, only only $2/24 = 0.0833$ of the incoming signal is correlated. In order to increase this rate, the SLC uses different combinations of all the other sub-correlations. In addition to this power increment, the combination achieves a narrower peak than the basic or even the autocorrelation functions.

One thing that has to be taken into account is the fact that the use of non-linear combinations increase the noise power. The following subsections presents the two new correlations.

1) SLC1: In [10] the authors presents the following combination of sub-correlations

$$
\begin{aligned}
R_{\cos}^{SLC1}(\tau) = & R_{\cos}^{Basic}(\tau) + \\
& \sum_{l=1}^{N_{cos}-2} \left(|R_{\cos}^l(\tau)| + |R_{\cos}^{Basic}(\tau)| - |R_{\cos}^l(\tau) - R_{\cos}^{Basic}(\tau)| \right)
\end{aligned} \quad (14)
$$

for BOCcos, where $N_{cos} = 4k$ and

$$
\begin{aligned}
R_{\sin}^{SLC1}(\tau) = & R_{\sin}^{Basic}(\tau) + \\
& \sum_{l=1}^{N_{sin}-2} \left(|R_{\sin}^l(\tau)| + |R_{\sin}^{Basic}(\tau)| - |R_{\sin}^l(\tau) - R_{\sin}^{Basic}(\tau)| \right)
\end{aligned} \quad (15)
$$

for BOCsin, $N_{sin} = 4k$.
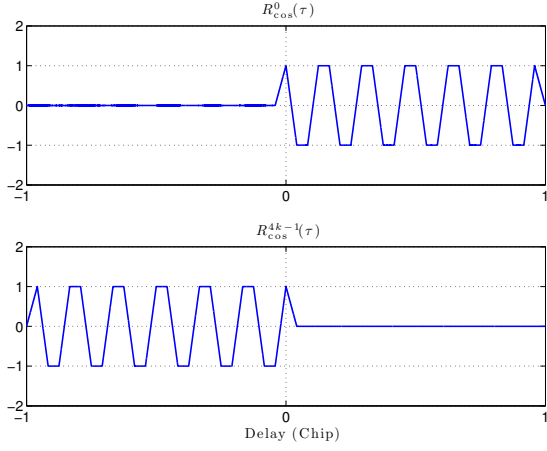
Fig. 4. First and last basic correlations for BOCcos(15,2.5) signal
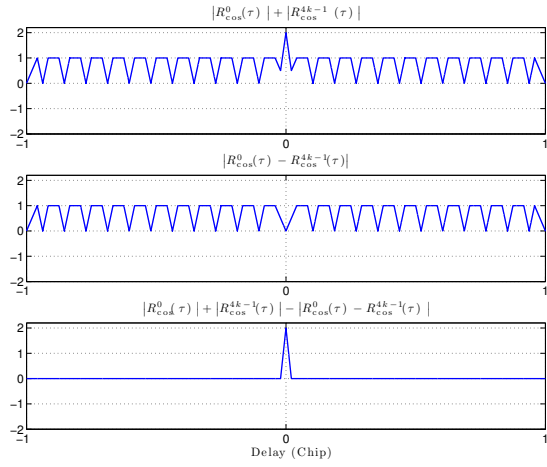
Fig. 5. Basic combination for a BOCcos(15,2.5)

the SLC1 method. It should be noted that, since the main lobe is narrower, the S-curve Gain is bigger. This is an advantage in terms of tacking variance, since the standard deviation depends inversely of the S-curve Gain.

Nevertheless, the slope of the main lobes of the SLC correlations is narrower than the matched filter, the noise is increased due to the non-linear combinations. The relation between the input power noise and the equivalent output power noise or the output SNR is not straightforward due to the non-linear combinations.
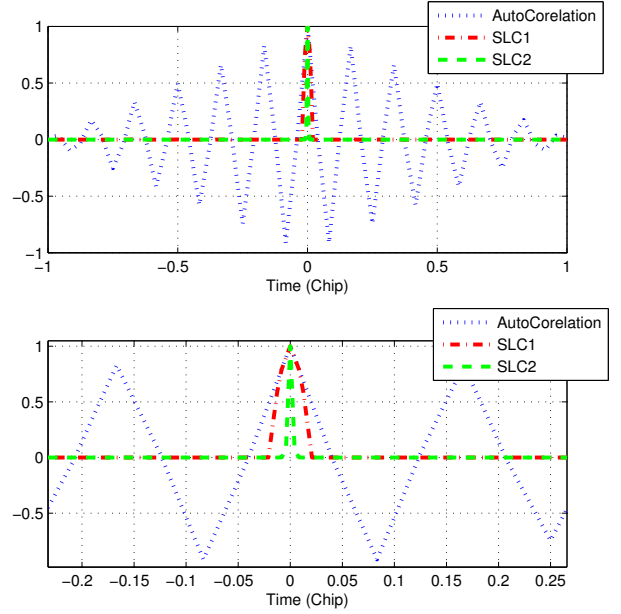
Fig. 6. Correlation of the SLC methods and the autocorrelation of the BOCcos(15,2.5)

2) SLC2 correlation: The second method ([8] and [11]) uses the same basic correlations than the SLC1 method. The difference is the combination between them. The authors use of the following combination

$$R_{\cos}^{SLC2}(\tau) = \prod_{q=0}^{2k-1} \left(\left| R_{\cos}^q(\tau) \right| + \left| R_{\cos}^{4k-q-1}(\tau) \right| - \left| R_{\cos}^q(\tau) - R_{\cos}^{4k-q-1}(\tau) \right| \right) \tag{16}$$

for BOCcos and

$$R_{\sin}^{SLC2}(\tau) = \prod_{q=0}^{k-1} \left(\left| R_{\cos}^q(\tau) \right| + \left| R_{\cos}^{2k-q-1}(\tau) \right| - \left| R_{\cos}^q(\tau) - R_{\cos}^{2k-q-1}(\tau) \right| \right) \tag{17}$$

for BOCsin.

The Fig.6 shows a comparison between the matched filter or the autocorrelation and the two SLC correlations presented in this section. At the top it can be seen how the SLC methods achieve an unambiguous correlation. The zoom of the main lobes can be observed at the bottom. The SLC2 method achieves a narrower lobe compared with the matched filter and

IV. PERFORMANCE COMPARISON

In this section, the two methods presented in this document are compared with the matched filter. The main features of the analysed signal are:

- Modulation: BOCcos(15,2.5)
- Subcarrier Frequency: 15.345 MHz
- Chip Rate: 2.5575 MHz
- $k = f_{sc} / f_c = 6$
- Code period: 0.01 seconds
- Number of chips: 25575

A. Noise in the SLC methods

In this section the noise effect in the SLC correlations is analyzed. By introducing noise in the signal, side lobes can appear. Fig.7 shows the effect caused by the noise in the SLC correlations, using 10^5 iterations, for different values of C/No. The SLC2 method seems to have a better behaviour than the SLC1 method, since it has only the side lobes closest to the principal. The lobes away from the main lobe are practically zero.
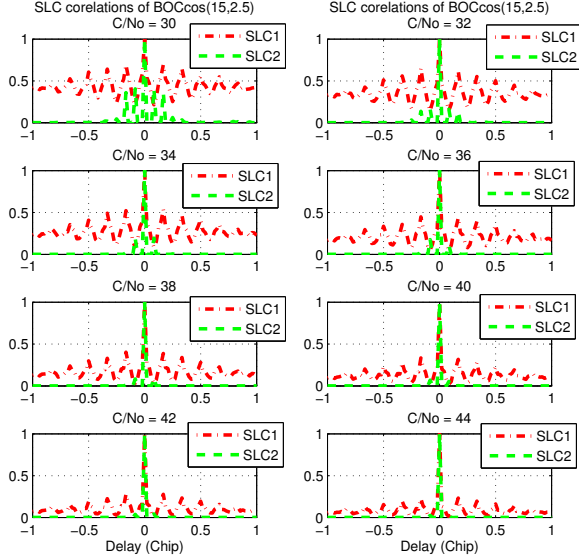
Fig. 7. Comparison between mean correlations of the SLC methods for different values of C/No

The Fig.8 shows twenty iterations of the SLC2 correlation for diferent values of C/No. It is noteworthy that the side lobes reappear again. In some iterations the value of a side lobe is bigger than the main one. The bigger the C/No is the smaller the side lobes are.
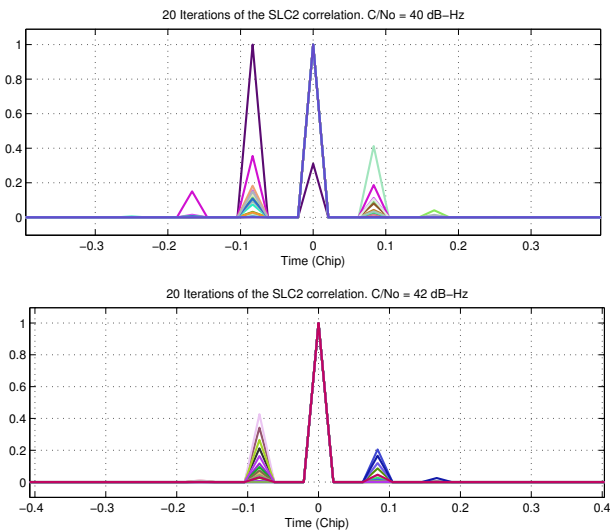
Fig. 8. Twenty iterations of the SLC2 correlation for $C/No = 40dB - Hz$ at the top and $C/No = 40dB - Hz$ at the bottom

B. Filter

Basically, two types of filters have been tested. The first one is a Butterworth filter, in which the group delay and phase delay are different. This kind of filters simulate the receiver filter [12]. The second one is a root cosine filter, which has both delays equals. In Fig.9 the response of both filters are shown.
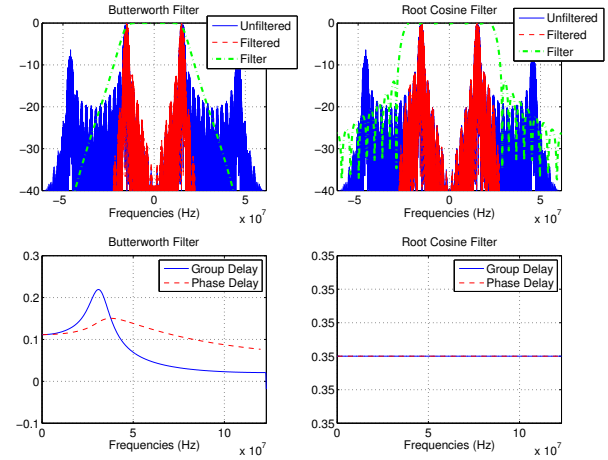
Fig. 9. Filters, phase delay and group delay

The filtered correlations are shown in Fig.10 and Fig.12. The results are quite interesting. In the first case, using a Butterworth filter, side lobes in both SLC correlations can be observed. Moreover, the Fig.11 shows that, the SLC1 correlation has not symmetric lobes. This could generate errors on the timing estimation, when it uses the early-minus-late method. Hence, the simulations show that, the new methods are ambiguous using filters with different delays (the filter phase delay and the filter group delay). It should be noted that, these simulations have been done without noise, the correlations are only afected by the filtering effect.

Only the SLC1 presents side lobes with the Root cosine filter. The SLC2 method remains unambiguous. Therefore, the SLC2 method seems to be more robust against asymmetries in the incoming signal or in the correlation.
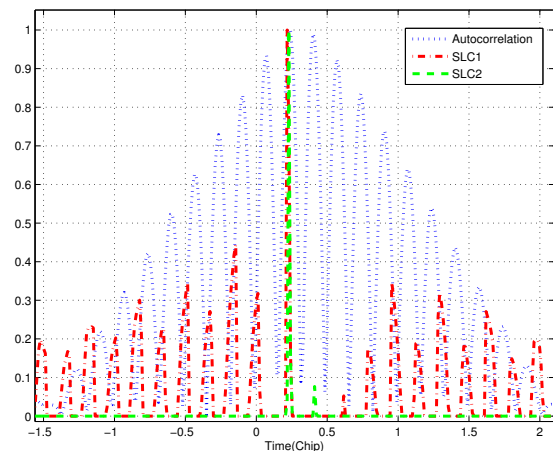
Fig. 10. Correlation using a Butterworth filter
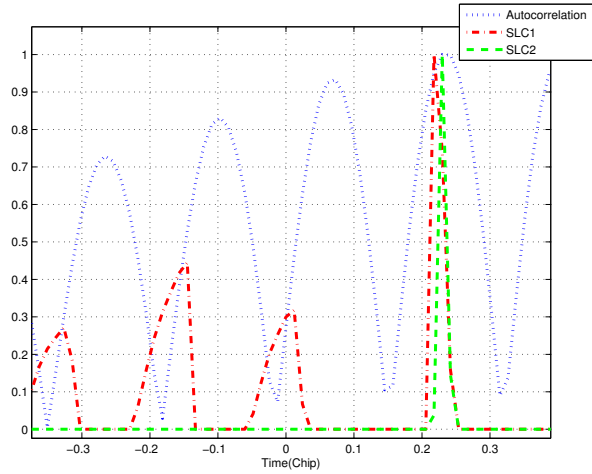
Fig. 11. Zoom of some lobes of the correlations using a Butterworth filter
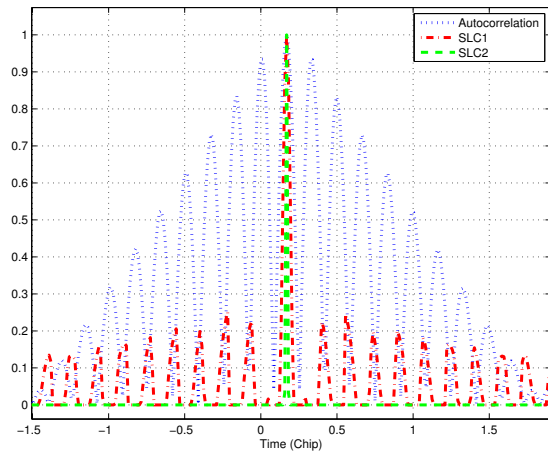
Fig. 12. Correlation using a FIR filter

C. Acquisition

In this section the results obtained in the acquisition process are presented. It can highlight two important results: the probability of signal detection and the probability of detecting the main lobe, once the signal has been detected (i.e. the false detection probability). Further, the thresholds have been defined through simulations. The closed expressions are valid only for the matched filter.

The thresholds have been designed through the Constant False Alarm (CFAR) criterion. This method sets the same P_{fa} for all values of C/No. The probability of false alarm has been set to 10^{-3} and it has been worked with the signal envelope. The threshold of the matched filter method can be found in [13]

$$V_t = \sigma\sqrt{-2lnP_{fa}} \qquad (18)$$

The detection probability for all the methods is shown in Fig.13. It can be seen that the new methods have worse

probability of detection than the matched filter. The SLC1 method loses about 2dB and the SLC2 loses about 4dB. This result was expected due to the non-linear operations introduced in the correlation. It should be noted that this probability includes the main and side lobes.
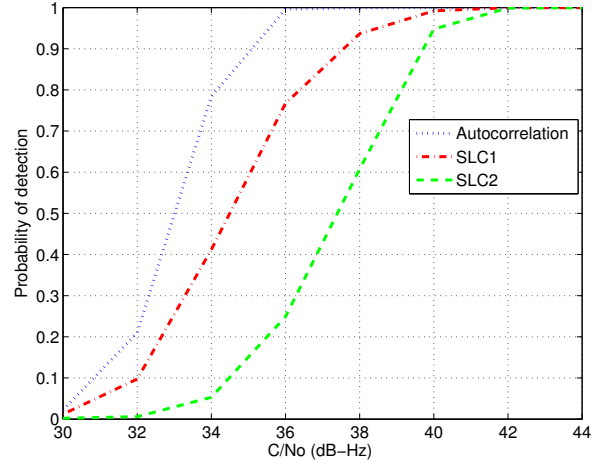
Fig. 13. Detection probability of SLC and traditional methods

The next step is to know the probability of detecting the main lobe. Once the signal has been detected, the probability of detecting the main or any side lobe is calculated (i.e the probability of false detection). The Fig.14 shows the probability of false detection. It can be seen that for the matched filter, the 10% of the detections a secondary lobule is detected for a C/No equal to 34dB. The SLC methods also have a probability of false detection different to zero for medium values of C/No. Theoretically, these methods were not ambiguous, but this simulation shows that when the signal is affected by noise it was not completely true.
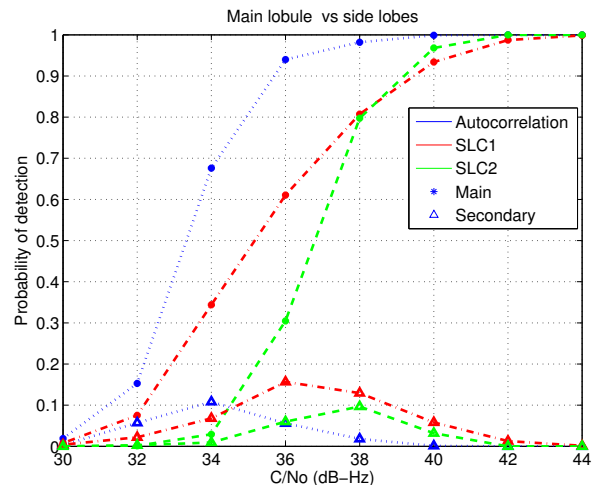
Fig. 14. False alarm probability of SLC and traditional methods

Method	Noise	Filters	Acquisition
SLC1	S.l. reappear	S.l. can reappear	P_d 4 dB less than traditional
SLC2	S.l. reappear	S.l. can reappear	P_d 3 dB less than traditional

TABLE I
SUMMARY OF THE BEHAVIOUR OF THE METHODS SLC

D. Tracking

The Fig.15 shows a comparison of the standard deviation between the autocorrelation and the SLC methods. In the first place, the standard deviation for the new two methods is somewhat higher than the matched filter. In the second place, the estimator has a non-linear behaviour for low values of C/No. The behaviour of the discriminator is not desired and the estimated value is biased.
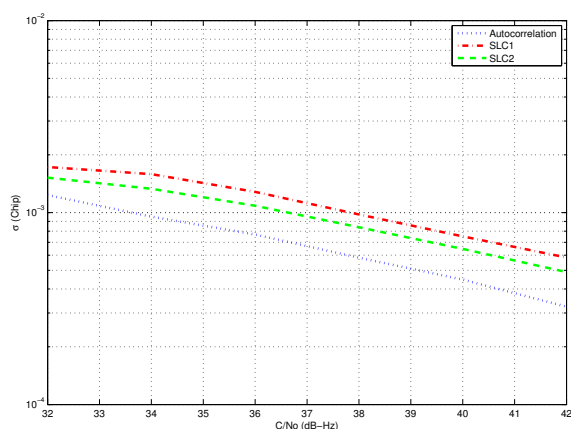
Fig. 15. Standard deviation of SLC and traditional methods using a non-coherent Early minus Late discriminator

The Table 1 shows the summary of the behaviour of the SLC methods for the different effects (S.l. means Side lobes).

V. CONCLUSION

In this document, the analysis of the two new side lobes cancellation techniques is presented. The SLC1 and SLC2 techniques are unambiguous and they consist in combining non-coherently different time slots of cross-correlation. The correlation obtained is much narrower than the matched filter. In principle, this is very beneficial feature of the SLC techniques. However, if noise is introduced, side lobes may grow again, especially for moderately low C/No (e.g. for 35dBHz in a GIOVE-A type signal). It is noteworthy to remark that, on average, the values of these peaks are lower than in the autocorrelation.

Due to the non-linear combinations of the partial correlations, the standard deviation increase considerably. In addition, the malfunction of the algorithm for low values of C/No has been shown, which produces a biased estimate because the estimator is saturated with noise. Moreover, it has been shown that, due to the reappearance of side lobes, the acquisition becomes ambiguous, achieving results even worse than the autocorrelation method. The probability of signal detection is worse compared to the autocorrelation case. In addition, due to the effect of noise there is a high probability of false detection, even higher than the autocorrelation case.

As a main conclusion, this type of correlation or discriminators seen to have strong limitations and the does not seem to be appropriate for high-order BOC signals due to the sensitivity to noise and distortion. For the time being, the three-loops methods seem to be the best option.

REFERENCES

[1] P. Fine and W. Wilso, "Tracking Algorithm for GPS Offset Carrier Signals," *Proceedings of the 1999 National Technical Meeting of The Institute of Navigation*, pp. 671–676, January 1999.

[2] P. Fishman and J. W. Betz, "Predicting Performance of Direct Acquisition for the M-Code Signal," *Proceedings of the 2000 National Technical Meeting of The Institute of Navigation*, pp. 574 – 582, January 2000.

[3] O. Julien, C. Macabiau, M. Cannon, and G. Lachapelle, "ASPeCT: Unambiguous sine-BOC(n,n) acquisition/tracking technique for navigation applications," *Aerospace and Electronic Systems, IEEE Transactions on*, vol. 43, no. 1, pp. 150–162, January 2007.

[4] Z. Yao, M. Lu, and Z. Feng, "Unambiguous sine-phased binary offset carrier modulated signal acquisition technique," *Wireless Communications, IEEE Transactions on*, vol. 9, no. 2, pp. 577–580, February 2010.

[5] M. Hodgart, P. Blunt, and M.Unwin, "Double estimator-a new receiver principle for tracking boc signals," in *.Inside GNSS*, 2008.

[6] J. Alegre-Rubio, C. Palestini, G. Lopez-Risueno, and G. Corazza, "Code Tracking of HighOrder BOC modulations in the Presence of Signal Distortion and Multipath," *5th European workshop on GNSS Signals and Singal Processing*, December 2011.

[7] S. Kim, S. Yoo, S. Yoon, and S. Y. Kim, "A Novel Unambiguous Multipath Mitigation Scheme for BOC(kn, n) Tracking in GNSS," in *Applications and the Internet Workshops, 2007. SAINT Workshops 2007. International Symposium on*, January 2007, p. 57.

[8] S. Kim, S. Yoo, S. H. Yoo, S. Y. Kim, and S. Yoon, "New Correlation Functions for CBOC Satellite Signal Synchronization," in *Advanced Communication Technology, 2008. ICACT 2008. 10th International Conference on*, vol. 2, February 2008, pp. 1045–1047.

[9] J. W. Betz, "Binary Offset Carrier modulations for radionavigation," *Institute of Navigation*, vol. 48, no. 4, pp. 227–246, Winter 2001-2002.

[10] Y. Lee, D. Chong, L. Song, S. Kim, G. Jee, and S. Yoon, "Cancellation of correlation side-peaks for unambiguous boc signal tracking." *IEEE Communications Letters*, vol. 16, pp. 569–572, 2012.

[11] S. Kim, S. Yoon, and S. Kim, "A Novel Multipath Mitigated Sidepeak Cancellation Scheme for BOC(kn, n) in GNSS," in *Advanced Communication Technology, The 9th International Conference on*, vol. 2, February 2007, pp. 1258 –1262.

[12] A. de Latour, T. Grelier, G. Artaud, and L. Ries, "Subcarrier tracking performances of BOC, ALTBOC and MBOC signals," in *ION GNSS*, 2007, pp. 769–781.

[13] E. D. Kaplan and C. Hegarty, *Understanding GPS: Principles and Applications*. Artech House Publishers, 2005.